



Optimization of pumping schemes for 160-Gb/s single channel Raman amplified systems

Xu, Lin; Rottwitt, Karsten; Peucheret, Christophe; Jeppesen, Palle

Published in:
I E E E Photonics Technology Letters

Link to article, DOI:
[10.1109/LPT.2003.820477](https://doi.org/10.1109/LPT.2003.820477)

Publication date:
2004

Document Version
Publisher's PDF, also known as Version of record

[Link back to DTU Orbit](#)

Citation (APA):
Xu, L., Rottwitt, K., Peucheret, C., & Jeppesen, P. (2004). Optimization of pumping schemes for 160-Gb/s single channel Raman amplified systems. *I E E E Photonics Technology Letters*, 16(1), 329-331.
<https://doi.org/10.1109/LPT.2003.820477>

General rights

Copyright and moral rights for the publications made accessible in the public portal are retained by the authors and/or other copyright owners and it is a condition of accessing publications that users recognise and abide by the legal requirements associated with these rights.

- Users may download and print one copy of any publication from the public portal for the purpose of private study or research.
- You may not further distribute the material or use it for any profit-making activity or commercial gain
- You may freely distribute the URL identifying the publication in the public portal

If you believe that this document breaches copyright please contact us providing details, and we will remove access to the work immediately and investigate your claim.

Optimization of Pumping Schemes for 160-Gb/s Single-Channel Raman Amplified Systems

Zhenbo Xu, Karsten Rottwitt, Christophe Peucheret, and Palle Jeppesen, *Member, IEEE*

Abstract—Three different distributed Raman amplification schemes—backward pumping, bidirectional pumping, and second-order pumping—are evaluated numerically for 160-Gb/s single-channel transmission. The same longest transmission distance of 2500 km is achieved for all three pumping methods with a 105-km span composed of superlarge effective area fiber and inverse dispersion fiber. For longest system reach, second-order pumping and backward pumping have larger pump power tolerance than bidirectional pumping, while the optimal span input signal power margin of second-order pumping is the largest and gets 5-dB improvement compared to backward pumping. Span loss tolerance increased to 140 km with more than 2000-km reach. Optimal signal power variation at both ends of the span can provide about 6-dB positive net gain.

Index Terms—Dispersion, noise, nonlinear optics, stimulated Raman scattering.

I. INTRODUCTION

DISTRIBUTED Raman amplification has emerged as a most attractive amplification scheme in recent research on 40-Gb/s wavelength-division multiplexing (WDM) transmission with merits of uniform gain profile and up to 10-THz dynamic operation bandwidth [1]. Pure Raman or hybrid Raman/erbium amplifications have been suggested [2], [3] as a way to improve the in-line signal to noise ratio in 160-Gb/s per-channel WDM systems compared to using lumped erbium-doped fiber amplifiers (EDFAs). Recent simulations indicate that symmetrical dispersion maps are favorable in case of distributed amplification [4]. Management of effective area and the noise performance have also been investigated in dispersion managed fiber spans [5], [6].

In this letter, we focus on 160-Gb/s single-channel systems and the use of Raman amplification. With realistic superlarge effective area (SLA) fiber and symmetrical dispersion map, we investigate three Raman pumping configurations—backward pumping, bidirectional pumping, and second-order pumping. In order to obtain a proper balance between nonlinearity and optical signal-to-noise ratio (OSNR), the signal evolution inside a span is adjusted by changing signal and pump power toward the maximum system reach. The pumping configuration characteristics and optimum span lengths for the systems are presented.

TABLE I
FIBER PARAMETERS

	D	S	n_2	Loss	A_{eff}	g_R	η
	(ps/nm/km)	(ps/km/nm ²)	(m ² /W)	dB/km	μm^2	(1/W/km)	(1/m)
SLA	20	0.06	2.23×10^{-20}	0.2	105	0.3	4×10^{-8}
IDF	-40	-0.12	2.37×10^{-20}	0.25	30	1.28	16.6×10^{-8}

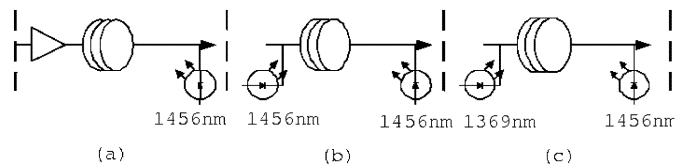


Fig. 1. Pumping configurations. (a) Backward pumping. (b) Bidirectional pumping. (c) Second-order bidirectional pumping.

II. RAMAN MODEL AND SYSTEM CONFIGURATIONS

A. Raman Model

In principle, the coupled wave equations give a simple description of Raman effect in the fiber [7]. Because of the large spectral width of a 160-Gb/s return-to-zero (RZ) signal, the coupled equations must include spontaneous Raman emission, Rayleigh backscattering, multiple Rayleigh backscattering, and intra-Raman effects within the signal spectrum. The Raman model we use considers all these effects [8]. The power evolution of each frequency component is calculated in an iterative way by coupling itself with all other frequency components propagating in the forward and backward direction into account. With respect to signal evolution in the time domain, the nonlinear Schrödinger equation (NLSE) is solved numerically using the split step method. In addition to dispersion, dispersion slope, and self-phase modulation (SPM), the NLSE also takes intrapulse Raman scattering and cross-phase modulation (XPM) effects into account, which are necessary for treating the short pulses used as the 160-Gb/s signals.

B. Simulation Parameters and Span Configurations

Transform-limited Gaussian pulses at 1552 nm with a full-width at half maximum of 1 ps are encoded with a PRBS length of 2^{10} [3] and launched into the transmission span. Symmetrical dispersion management is used with 35-km SLA fiber at both ends and 35 km inverse dispersion fiber (IDF) in the middle of the span. Table I gives the values of the fiber parameters for the SLA and IDF. Here, D is the dispersion, S the dispersion slope, n_2 the nonlinear index, A_{eff} the effective area, g_R the Raman gain coefficient, and η the Rayleigh backscattering coefficient. For simplicity we assume that the nonlinear index, fiber loss, and effective area are wavelength independent.

Manuscript received July 8, 2003.

The authors are with COM, Technical University of Denmark, DK-2800 Kgs. Lyngby, Denmark (e-mail: xuz@com.dtu.dk).

Digital Object Identifier 10.1109/LPT.2003.820477

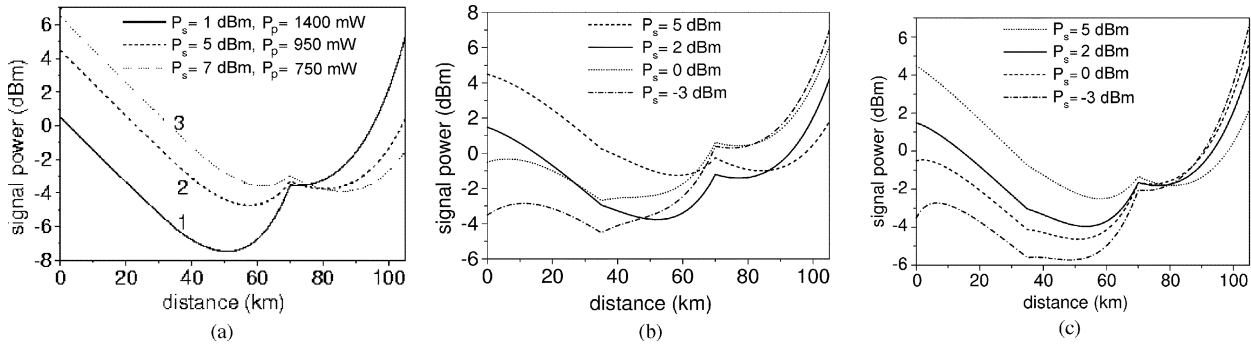


Fig. 2. Signal power evolution in a 105-km span for: (a) backward pumping; (b) bidirectional pumping; and (c) second-order bidirectional pumping. The pump powers in (b) and (c) have been set to maximize the transmission distance for -3 , 0 , 2 , and 5 -dBm span input signal power, respectively.

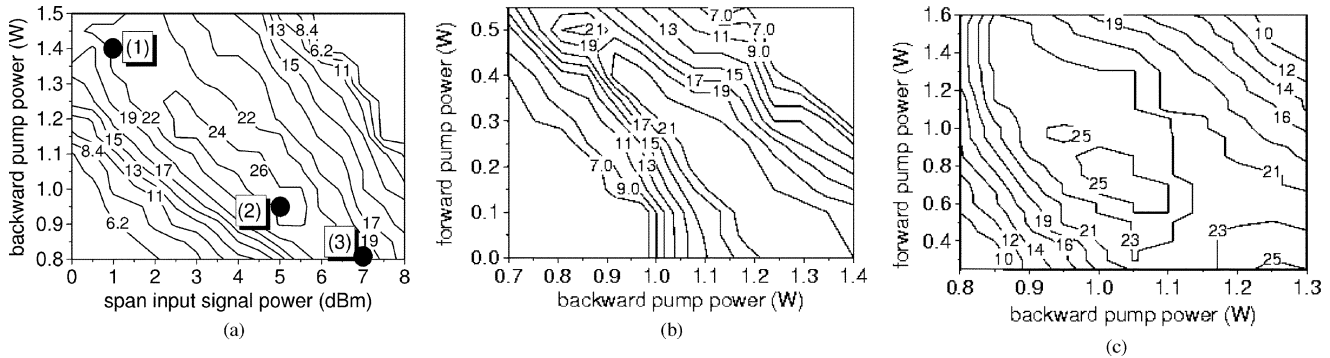


Fig. 3. Number of transmitted 105-km spans as a function of: (a) span input signal power and pump power for backward pumping; (b) backward and forward pump power for bidirectional pumping; and (c) backward and forward pump power for second-order bidirectional pumping.

A third-order Gaussian optical filter with 5-nm bandwidth and a 110-GHz bandwidth electrical Bessel filter are used at the receiver. An analytical fit to the Raman gain response of pure silica fiber [7] is used, with accurate experimental values for the gain peaks in the SLA and IDF.

The three Raman pump configurations are illustrated in Fig. 1. For backward pumping, the pump is placed at the end of the span, while an EDFA with 5-dB noise figure is used at the input. The bidirectional pumping scheme uses two pumps at 1456-nm wavelength, whereas in the second-order pumping configuration a backward pump at 1456 nm and a forward pump at 1369 nm are used.

III. RESULTS

For all the results presented below, a bit error rate (BER) of 10^{-9} is taken as the criterion for defining the maximum system reach.

Fig. 2 shows the optimal signal power evolution resulting in the longest system reach for all three pumping configurations, while Fig. 3 shows the systems reach contours as a function of signal and pump power for each pump configuration. In Fig. 2(a), curves 1, 2, and 3 correspond to the three sets of span input signal power and backward pump power indicated with points in Fig. 3(a). Curve 2 presents the signal power distribution along the fiber span for longest system reach. Curve 1 and 3 present signal power distributions in case of 15% degradation of the system reach. Curve 3 is expected to result in less nonlinearity accumulation compared to curve 2, but the system reach is degraded due to reduction in OSNR stemming from more

Raman-induced noise. This suggests the existence of a minimum signal power limit in the power distribution. Curve 1 corresponds to less Raman-induced noise because of lower pump power, but nonlinearity accumulation is higher than for curve 2 and becomes the limiting factor. Hence, there is also an upper limit for the signal power distribution set by nonlinearities. The optimized signal power evolutions for longest reach are also shown in Fig. 2(b) and (c) for bidirectional and second-order pumping at different input signal power, respectively.

For all investigated pumping configurations and signal input power levels, it can be seen that the signal power has to remain above -6 dBm within the span to get optimal results. In all optimal system reach cases, although large signal power variations can be tolerated in both SLAs, the lowest signal power in the span is reached within the IDF. Therefore, there is a tradeoff between OSNR and nonlinearity, which means the IDF constitutes a nonlinearity bottleneck in the system.

For all the pumping configurations, about the same optimal longest distance of 2500 km is reached. From Fig. 3, we define the optimal power operation range for the three pumping configurations to be within 15% shorter reach compared to the maximum transmitted distance of 2500 km, i.e. in the 2200–2500-km range. In the backward pumping case, the optimum pumping power range is 200 mW. However, for bidirectional pumping, both pump power levels are much more critical; the tolerance of the optimum range for both pump powers decreases from 200 to 100 mW. In the second-order pumping case, the pump power tolerance is the largest, namely, more than 200 mW for the backward pump power and more than 600 mW for the forward pump power.

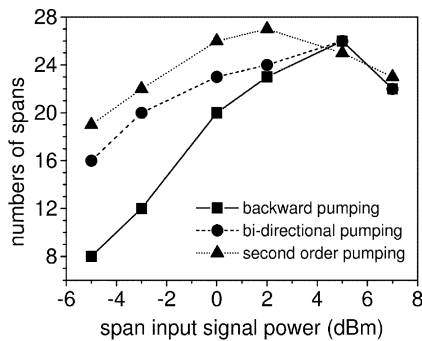


Fig. 4. Maximum transmitted spans as a function of span input signal power. Span length is 105 km.

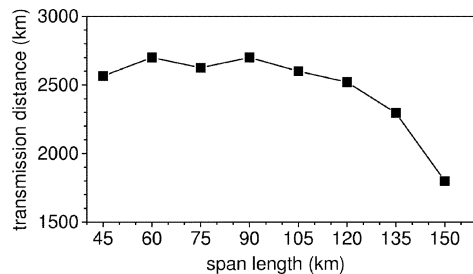


Fig. 5. Transmission distance versus span length for backward pumping.

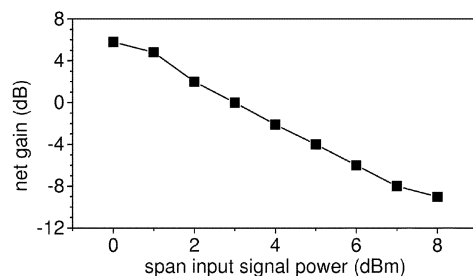


Fig. 6. Net-gain versus span input signal power for backward pumping with 105-km span length.

For both bidirectional and second-order pumping, extensive calculations have been performed of longest transmission distance for different span input signal power levels. The results are shown in Fig. 4. It is clear from Fig. 4 that backward pumping is most sensitive to decreasing incident signal power due to OSNR limitations, while second-order pumping offers large tolerance to decreasing signal power. Above 2200-km system reach, second-order pumping can accept around 9 dB span input signal power variation, while for bidirectional and backward pumping it is limited to 5 and 3 dB. The results from Figs. 3 and 4 indicate that for a single-channel system, backward pumping has acceptable pump power margin; it is also the simplest and most practical pumping scheme. Second-order pumping offers the largest pump and span input signal power tolerance. Furthermore, it has good potential for being used in WDM transmission at 160 Gb/s because it allows lower incident signal power, which mitigates nonlinear degradation between channels. On the other hand, it is also a more costly pumping scheme.

Since backward pumping has good performance and is the simplest and most cost-effective pumping scheme, we focus on backward pumping in the following.

We now investigate the influence of span length on the system reach by scaling the fiber length linearly without changing any other fiber parameters. From Fig. 5 it is clear that the longest transmission distances have large span length tolerance. The span length can be increased from 45 to 120 km while maintaining a system reach above 2500 km. The large span loss tolerance is very beneficial for practical designs.

The signal net gain, defined as the ratio between output and input signal power, was also investigated. For each incident signal power in case of optimum system reach, the net gain as a function of span input signal power is shown in Fig. 6. The data are collected from the power contour in Fig. 2(a). More than 6 dB positive net gain can be realized while still maintaining good performance, which means that placing an EDFA before the span is not necessary; instead, the positive net gain can be used to compensate insertion loss between the spans.

IV. CONCLUSION

In conclusion, 160-Gb/s single-channel transmission using a scheme consisting of two SLA fibers separated by an IDF and Raman amplification has been investigated numerically. Backward pumping, bidirectional pumping, and second-order pumping were investigated. For the three schemes, about the same systems reach of 2500 km was obtained. For the single-channel system considered, backward pumping is not only the simplest configuration, but it also offers good pump power margin. Second-order pumping shows largest pump power and input signal power tolerance. All three configurations offer a span length tolerance of 45 to 135 km and positive net gain can be obtained. Second-order pumping could be more attractive for WDM applications because it allows lower input power levels that would mitigate the influence of nonlinearities.

REFERENCES

- [1] B. Zhu, L. Nelson, L. Leng, S. Stulz, M. Pedersen, and D. Peckham, "Transmission of 1.6 Tb/s (40×42.7 Gb/s) over transoceanic distance with terrestrial 100-km amplifier spans," in *Tech. Dig. Opt. Fiber Commun. Conf., OFC'03*, vol. 2, 2003, paper FN2, pp. 742–743.
- [2] B. Mikkelsen, G. Raybon, B. Zhu, R. J. Essiambre, P. G. Bernasconi, K. Dreyer, L. W. Stulz, and S. N. Knudsen, "High spectral efficiency (0.53 bit/s/Hz) WDM transmission of 160 Gb/s per wavelength over 400 km of fiber," in *Tech. Dig. Opt. Fiber Commun. Conf., OFC'01*, Anaheim, CA, 2001, Paper ThF2.
- [3] B. Cuenot, "Comparison of engineering scenarios for $N \times 160$ Gb/s WDM transmission systems," *IEEE Photon. Technol. Lett.*, vol. 15, pp. 864–866, June 2002.
- [4] R. Hainberger, T. Hoshida, T. Terahara, and H. Onaka, "Comparison of span configurations of Raman-amplified dispersion-managed fibers," *IEEE Photon. Technol. Lett.*, vol. 14, pp. 471–473, Apr. 2002.
- [5] M. Vasilyev, "Raman-assisted transmission: toward ideal distributed amplification," in *Tech. Dig. Opt. Fiber Commun. Conf., OFC'03*, vol. 1, 2003, Paper WB1, pp. 303–305.
- [6] A. Kobayakov and M. Vasilyev, "Performance analysis of Raman amplifiers based on dispersion-managed fibers," in *Tech. Dig. Opt. Fiber Commun. Conf., OFC'03*, vol. 1, 2003, Paper WB2, pp. 305–306.
- [7] G. P. Agrawal, *Nonlinear Fiber Optics*. San Diego, CA: Academic, 2001.
- [8] H. Kidorf, K. Rottwitt, M. Nissov, M. Ma, and E. Rabarjaona, "Pump interaction in a 100-nm bandwidth Raman amplifier," *IEEE Photon. Technol. Lett.*, vol. 11, pp. 530–532, Nov. 1999.